

# Modeling Internal Tides and Mixing Over Ocean Ridges

Donald Slinn<sup>1</sup>, Murray D. Levine<sup>2</sup>

<sup>1</sup> Department of Civil and Coastal Engineering, University of Florida, Gainesville, Florida • <sup>2</sup> College of Oceanic and Atmospheric Sciences, Oregon State University, Corvallis, Oregon

AGU Fall Meeting 2002 • Poster OS11C-0236

## BACKGROUND

The location, strength, and mechanisms that produce sufficient vertical mixing in the ocean to balance the large-scale thermohaline circulation are not well understood. The NSF has dedicated significant resources to increase understanding of the role of tidally induced mixing in benthic boundary layers in the Hawaiian Ocean Mixing Experiment (HOME).

One of the three goals of the HOME program is: “to determine the principal mechanisms which transfer energy from large scale flows to turbulent motions. Do these mechanisms work differently in the deep sea and the upper ocean? How do the depth and lateral dependencies of  $K_\rho$  depend on characteristics of the topography and the tides? These findings will support generalization of HOME observations throughout the Ridge and to the global ocean.” (Pinkel et al., 1998)

HOME data show that nearly barotropic tides over steep ocean slopes can produce regions of shear instabilities that cause turbulent mixing. We pursue improved understanding of tidally induced mixing by comparing field observations to numerical experiments.

## FIELD OBSERVATIONS

Levine and Tim Boyd (OSU) are investigating the energy pathway from barotropic tide to internal tide to enhanced diapycnal mixing. They deployed a mooring with vertical arrays of temperature and conductivity sensors and an upward looking ADCP for 2 months over the flank of a steep ridge (with a rise of 1.3 km in 10 km) in 1450 m of water about 50 km off Oahu. The location of the measurements were ideally situated to capture interactions of the nearly barotropic tide with the sloping topography. The major axis of the barotropic tidal current is 10-20 cm/s and is aligned almost directly cross-slope over a relatively smooth, two-dimensional section of the ridge.

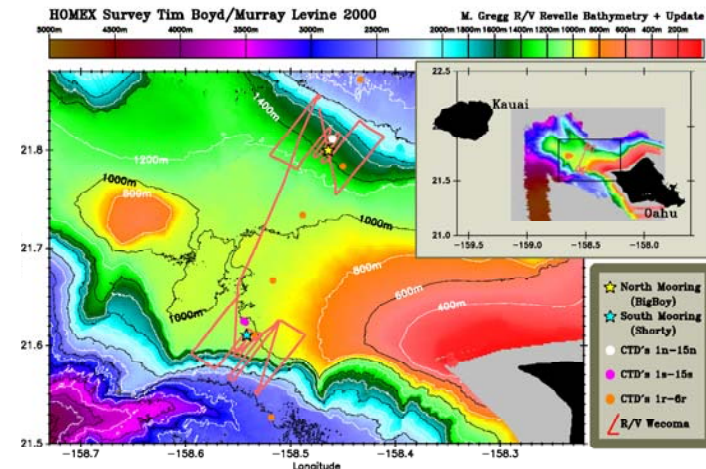
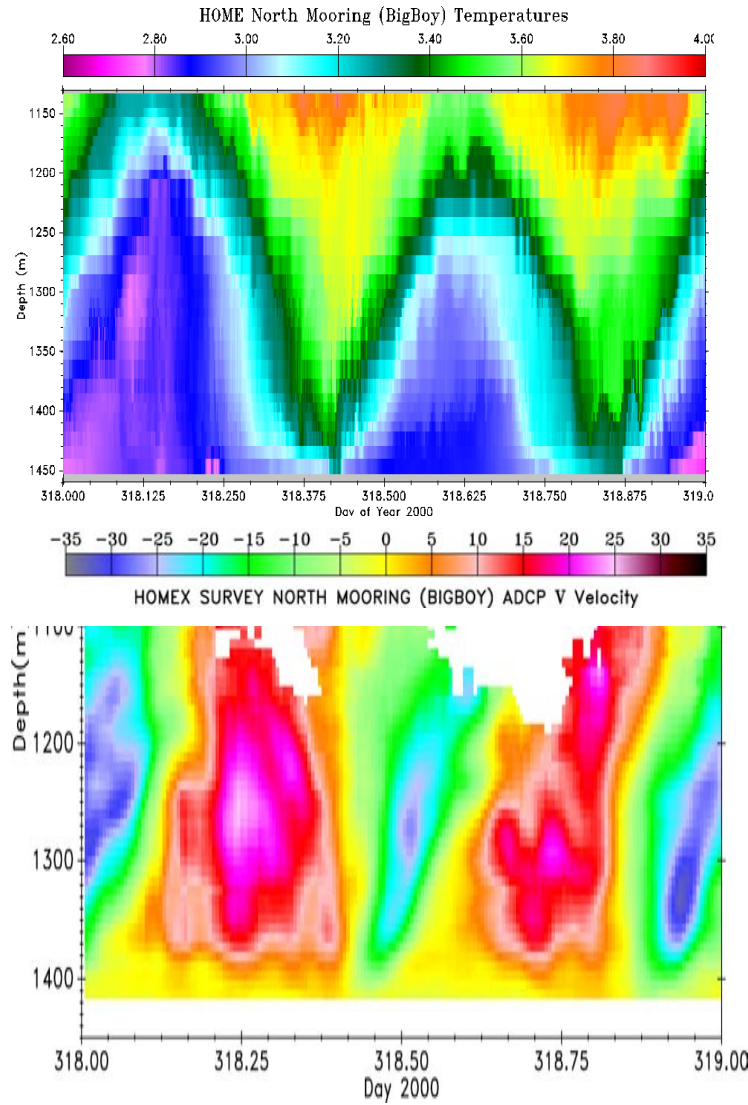


Figure 1. Mooring location on Hawaiian Ridge.



**Figure 2.** Time series of temperature and upslope velocity over two tidal periods from the moored measurements at the “Big Boy” site in the HOME.

## MODEL FORMULATION

In our approach, we use the Navier Stokes equations with the  $f$ -plane and Boussinesq approximations on a long, smooth slope. We write the non-dimensionalized equations of motion in a rotating and rotated (about the  $y$ -axis) reference frame. Here,  $\alpha$  is the bottom slope;  $u$  and  $x$  are upslope;  $v$  and  $y$  are across or along the slope; and  $w$  and  $z$  are normal to the slope, such that gravity has a component in both the  $x$  and  $z$  directions. Our model is designed for both DNS and LES. Here we present model results at moderate Reynolds number (30,000 – 80,000) using a constant-eddy viscosity diffusion model (DNS) because the results are dependent on the boundary layer interactions near the wall.

$$\begin{aligned} \frac{\partial u}{\partial t} + \vec{u} \cdot \nabla u + Ri \rho \sin \alpha &= -\frac{\partial p}{\partial x} + \frac{\partial \tau_{1k}}{\partial x_k} + \frac{1}{Ro} v \cos \alpha \\ \frac{\partial v}{\partial t} + \vec{u} \cdot \nabla v &= -\frac{\partial p}{\partial y} + \frac{\partial \tau_{2k}}{\partial x_k} - \frac{1}{Ro} [u \cos \alpha - w \sin \alpha] \\ \frac{\partial w}{\partial t} + \vec{u} \cdot \nabla w + Ri \rho \cos \alpha &= -\frac{\partial p}{\partial z} + \frac{\partial \tau_{3k}}{\partial x_k} - \frac{1}{Ro} v \sin \alpha, \\ \frac{\partial \rho}{\partial t} + \vec{u} \cdot \nabla \rho &= \frac{\partial \tau_{\rho k}}{\partial x_k} + w \cos \alpha + u \sin \alpha \\ \frac{\partial u}{\partial x} + \frac{\partial v}{\partial y} + \frac{\partial w}{\partial z} &= 0 \end{aligned}$$

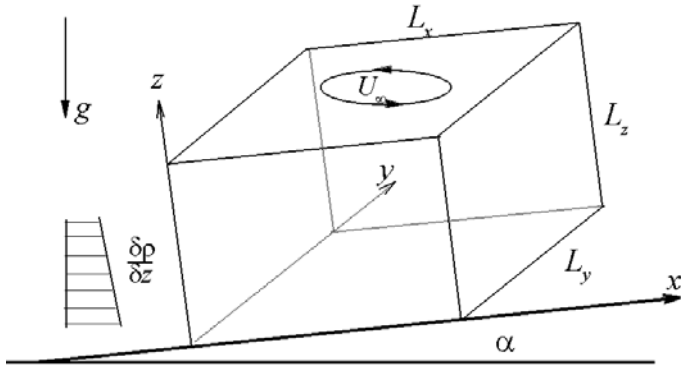


**Figure 4.** Model geometry, simulations conducted on a periodic control volume on a slope with a constant background density gradient and tidal forcing produced by a barotropic pressure gradient;  $U = U_M \cos(\omega t)$  where  $\omega = 2\pi / T_p$  is the tidal frequency..

## MODEL COMPARISON

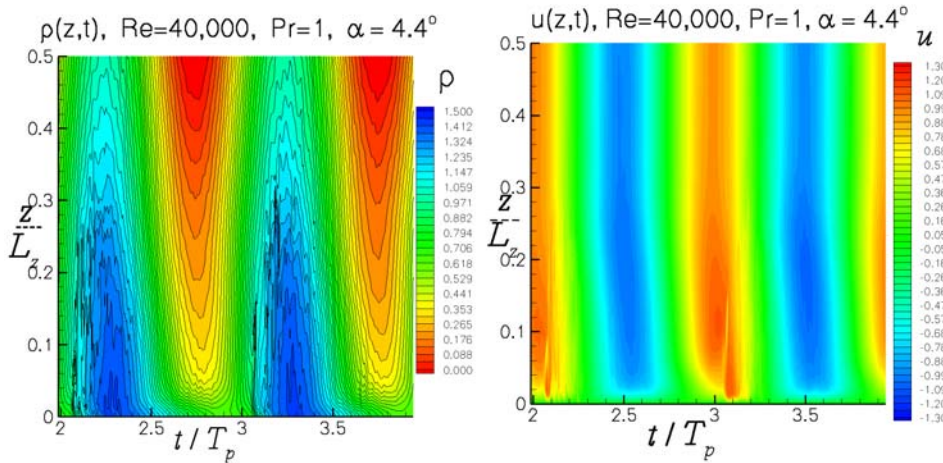


**Figure 3.** Time series of density field and upslope velocity over 2 tidal periods from model simulations.

## MODEL PARAMETERS

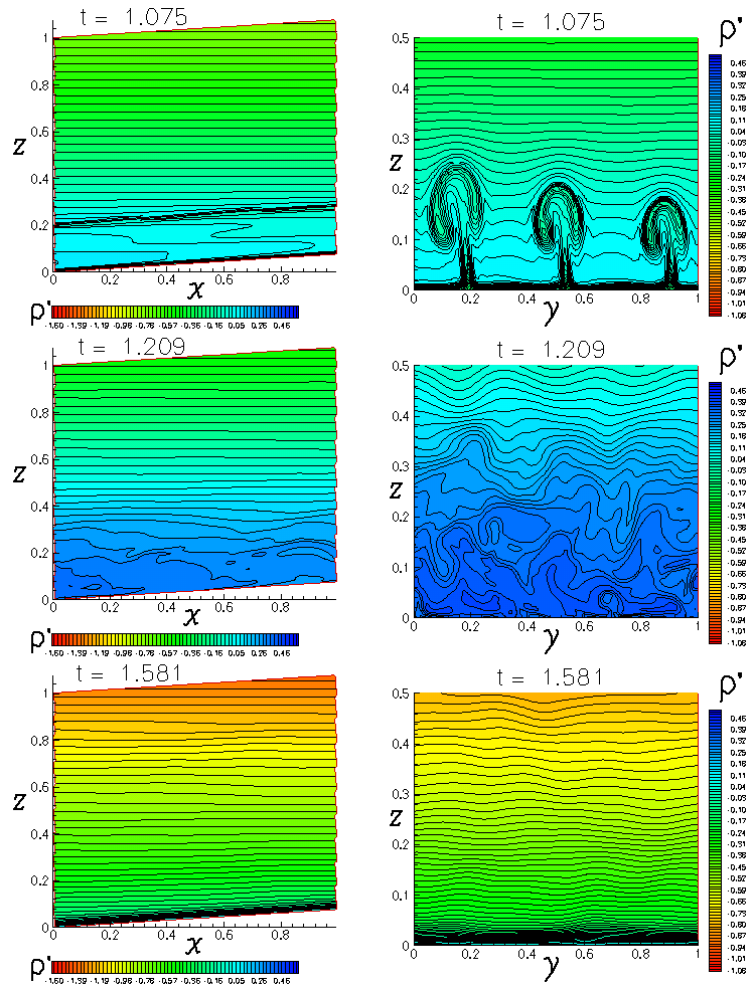
Physical parameters used in the simulations are taken from the field measurements, e.g.,  $N = 2.2 \times 10^{-3} \text{ s}^{-1} = 1.25 \text{ cph}$ , the latitude is  $21.8^\circ \text{ N}$ , for a Coriolis parameter of  $2.7 \times 10^{-5} \text{ s}^{-1}$ , and the tidal period of the M2 tide is 12.4 hours. We have non-dimensionalized the velocity fields by the maximum tidally induced velocity,  $U = U_M (= 20 \text{ cm/s})$ , scaled time by  $U/L$ , the lengths by the vertical domain size (i.e.,  $L = L_z = 200 \text{ m}$ ), and the density field by the background density gradient.  $Ro = U/fL$  is the Rossby number and  $Ri = (NL/U)^2$  is the Richardson number. These yield a background Richardson number of 4.84 and a Rossby number of 37.

The bottom boundary is a rigid sloping wall ( $0 < \alpha < 9^\circ$ ) satisfying the “no-slip” boundary condition, while the top boundary is a fixed rigid lid allowing “free-slip” conditions. The bottom boundary has a no-flux condition on the density field, and the top boundary is an open boundary with the density gradient held equal to the background. The four horizontal boundaries of the domain are periodic. We use  $129 \times 129 \times 150$  ( $n_x \times n_y \times n_z$ ) grid points for a domain size of  $[L_x, L_y, L_z] = [200, 200, 200] \text{ m}$ , with a constant viscosity on the order of  $10^{-4} \text{ m}^2 \text{ s}^{-1}$ .

## INTRODUCTORY RESULTS

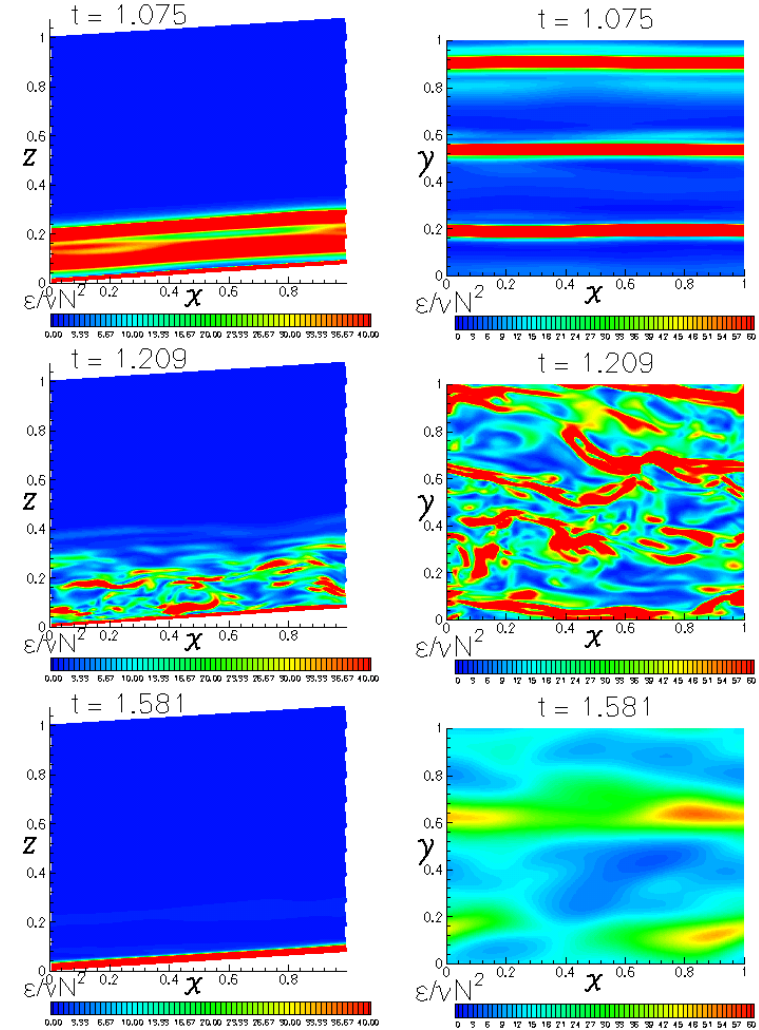
We examined flow response to 4 key parameters:

- Bottom Slope,  $\alpha$
- Reynolds Number,  $Re$
- Prandtl Number,  $Pr$
- Rossby Number,  $Ro$



**Figures 5.** Side and end views of Isopycnals during three phases of flow development, at the onset of turbulence, during the height of mixing, and laminar phase during down-slope flow.

## RESULTS



**Figures 6.** Contours of the kinetic energy dissipation rate normalized by  $n N^2$  during the same three phases of the flow, side view and top view, showing complex turbulent structure.



## RESULTS

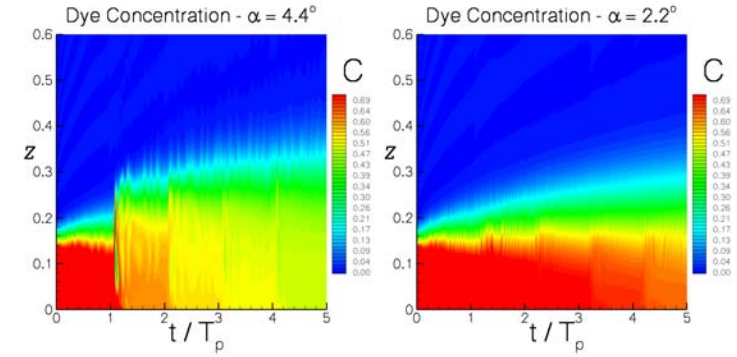


**Figure 9.** Horizontally averaged dye concentration as a function of time shows different levels of turbulent mixing across the boundary layer.

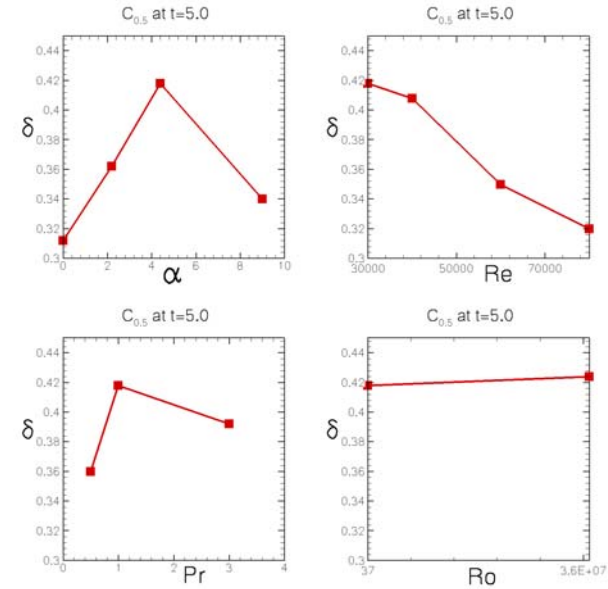


**Figure 10.** Upper interface of the Dye layer (where concentration is 0.05 at  $t = 5.0$  tide periods), as a function of bottom slope, Reynolds, Prandtl ( $\nu / k$ ), and Rossby numbers.

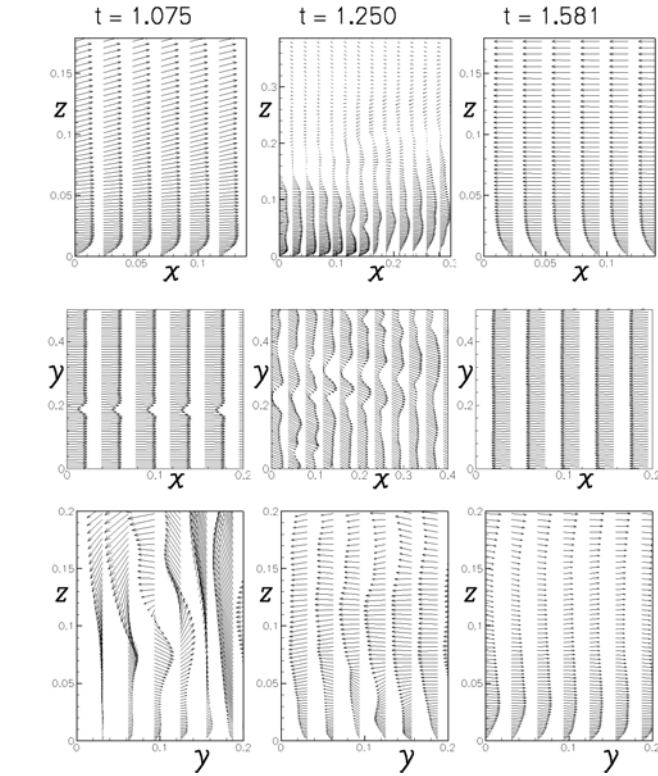


**Figure 7.** Velocity vectors in the near wall region, side, top and end views at different phases of the mixing cycle.

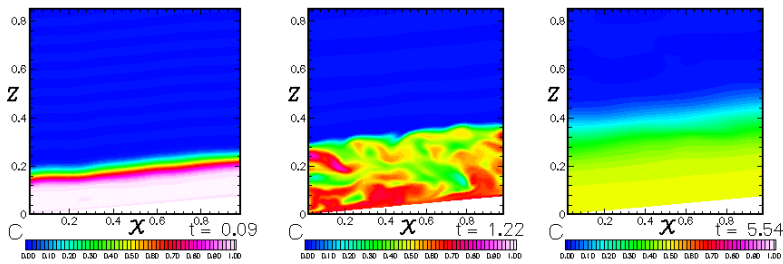


**Figure 8.** Cross sections of concentration of Dye field in tracer release experiments for  $\alpha=4^\circ$ ,  $Re=40,000$ ,  $Pr=1$ .

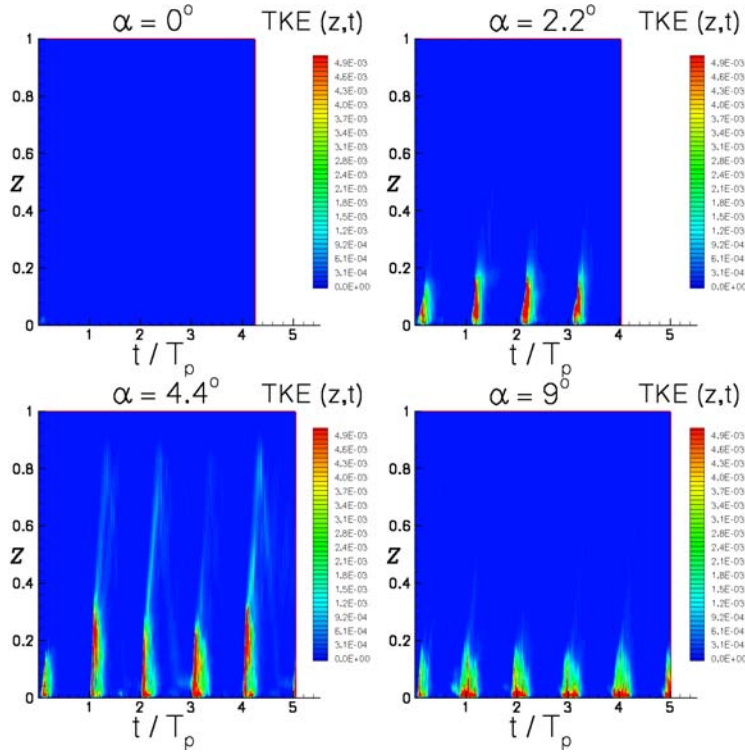


**Figure 11.** Horizontally averaged turbulent kinetic energy as a function of time for different bottom slopes at  $Re=30,000$ ,  $Pr=1$ . Note that the turbulence begins sooner for the steeper slope.

When the barotropic tidal flow is upslope, the stratification near the boundary is greatly reduced and denser deep water is advected above the less dense water retained in the boundary layer. This leads to statically unstable situations and plumes rise from the wall and produce persistent strong mixing events that are several tens of meters thick and last for approximately one quarter of the tidal period. Conversely, during the down-slope tidal flow, denser fluid remains trapped in the boundary layer as less dense upslope fluid is advected downward, leading to very strong stratification near the boundary, which shuts down vertical mixing over the slope. The rate at which light water is over-run by deeper water is related to the momentum thickness of the turbulent boundary layer (the thickness of a hypothetical layer moving at the free-stream velocity having equivalent momentum to the velocity deficit of the boundary layer):

$$\theta(t) = \int_0^\delta \frac{u}{U_\infty} \left( 1 - \frac{u}{U_\infty} \right) dz$$

For (unstratified) turbulent flows  $\theta \approx 0.1\delta$  while for laminar flows  $\theta \approx 0.15\delta$ .

Production of unstably stratified water

(potential energy) per unit width goes as:  $PE = g \int_v \rho z dv$

And the rate of diapycnal mixing is proportional to:

$$R_f \beta A_{xy} g \frac{\theta^2}{2} U \frac{\partial \bar{\rho}}{\partial z} \sin(\alpha)$$

Here  $\beta$  is the factor accounting for the angle between the principal axis of the barotropic tide and the upslope direction.

$A_{xy}$  is the planform area, and  $R_f \sim 0.2$  is the mixing efficiency, the percentage of displaced variable density fluid that undergoes irreversible mixing, rather than rising through the layer of heavier fluid intact and returning to its mean resting level above the boundary layer. As turbulence increases,  $R_f$  should increase.

It appears that the production of diapycnal mixing in the benthic boundary layer by this process may be quite large, and nearly ubiquitous on slopes.

## *KEY OBSERVATIONS*

A previously unconsidered process offers a physically plausible explanation for some portion of turbulent mixing on benthic slopes.

- With lengths scaled by the density gradient, we predict boundary layers approximately 100 m thick.
- The 4° slope produces the highest levels of turbulence and the thickest boundary layers in our simulations, this may be related to at least 3 factors:

For the given background stratification the tidal frequency is near critical for this slope.

At smaller slopes less potential energy is produced.

At larger slopes the buoyant water is released from the boundary layer earlier in the tidal phase, yielding longer duration, less intense mixing.

- The buoyant plumes are initially very two-dimensional, aligned in the upslope flow direction suggesting a strong inhibition of the Rayleigh-Taylor instability by the mean shear.
- There is a very strong asymmetry in the process during the different phases of the tide. During down-slope flow increased stratification near the boundary inhibits turbulence in the benthic boundary layer.

## *FUTURE WORK*

Our ongoing efforts are focusing on:

- Large Eddy Simulations at higher Reynolds numbers.
- Quantification of the net mixing (using Lagrangian tracers and Thorpe displacements).
- Examination of the influence of wall models for stratified turbulence.
- Comparison with field data from HOME.
- Increased realism in the model, including time dependent global straining of the background density field in the vicinity of the bottom topography.